Title

Assessing marine communities and carbon cycling that sustained shallow-marine ecosystems on Silurian, reef-rimmed carbonate platforms

Authors

Marshall, Nathan L
Love, Gordon D
Grytsenko, Volodymyr
et al.

Publication Date

2023

DOI

10.1016/j.orggeochem.2022.104528

Peer reviewed

Organic Geochemistry 175 (2023) 104528

Contents lists available at ScienceDirect

Organic Geochemistry

journal homepage: www.elsevier.com/locate/orggeochem

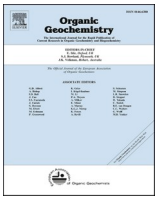

Assessing marine communities and carbon cycling that sustained shallow-marine ecosystems on Silurian, reef-rimmed carbonate platforms

Nathan L. Marshall [a,*], Gordon D. Love [a], Volodymyr Grytsenko [b], Andrey Bekker [a,c]

[a] Department of Earth & Planetary Sciences, University of California, Riverside, 900 University Avenue, Riverside CA 92521, USA
[b] Geological Museum of the State Natural History Museum, National Academy of Sciences, 15 B. Khmelnitsky Str., 01030 Kyiv, Ukraine
[c] Department of Geology, University of Johannesburg, Auckland Park, Johannesburg 2006, South Africa

ARTICLE INFO

Associate Editor-Julian Sachs

Keywords:
Silurian
Green algae
Reef-rimmed carbonate platform
3β-Methylhopane
Methane cycling

ABSTRACT

A detailed middle Silurian to Early Devonian biomarker stratigraphic record was obtained from thermally well-preserved strata, sampled from a > 400 m long drill-core 25 from Podillya, Ukraine, deposited in the Podillyan *peri*-continental basin. These lipid biomarker records provide useful insights into the temporal changes in microbial ecology and ocean chemistry for this ancient, tropical shallow-marine reefal carbonate platform. The paleoenvironmental conditions favored sustenance of bacteria over algae (as indicated by elevated hopane/sterane ratios (average: 10.7, maximum value of 36.9); and appreciable 2α-methylhopanes and 3β-methylhopanes) in this nutrient-depleted, marine reefal habitat. The setting behind the reef tract in a lagoon and muted nutrient supply from the open ocean likely contributed to the persistently low primary productivity and low net biomass over millions of years of deposition. The most prolific algal primary producers were green algae consistent with a C_{29} sterane dominance. No detectable contributions of 24-*n*-propylcholestane (24-npc) and/or other C_{30} regular sterane compounds were found with GC–MRM-MS. Elevated 3β-methylhopane index values (3-MeHI; range: 3–13%, mean: 6.4%) were observed throughout the core interval, which is a characteristic associated with source contributions from methanotrophic bacteria and indicative of an enhanced marine methane cycle. This extends the previous findings of consistently high abundances of 3-methylhopanes for Ordovician marine environments to include a tropical, marine shelf setting persisting through the Silurian Period.

1. Introduction

The Silurian Period (443.8–419.2 Ma) was once regarded as an interval of relative climatic and environmental stability during a greenhouse climate (Fisher, 1982; Bassett et al., 1990; Johnson, 1991). However, more recent biostratigraphic and chemostratigraphic investigations have demonstrated that changes in the global climate and marine carbon cycling during the Silurian Period were more frequent and dramatic than previously recognized, with at least four major global-scale carbonate $\delta^{13}C$ ($\delta^{13}C_{carb}$) excursions (> +4‰) identified (Jeppsson, 1990; Calner, 2008; Munnecke et al., 2010; Vandenbroucke et al., 2015; Hartke et al., 2021). These positive carbon isotope excursions are all closely associated with major faunal turnover events in both the benthic and pelagic marine realms. Biogeochemical models and various geochemical proxies have provided independent evidence that one of the most dramatic Phanerozoic rises in atmospheric and marine O_2 concentrations likely occurred through the Silurian Period and perhaps continued well into the Silurian–Devonian transition (Berner and Canfield, 1989; Berner, 2009; Krause et al., 2018; Stolper and Bucholz, 2019; Sperling et al., 2021). Thus far though, the precise trajectory of the rise of atmospheric and marine O_2 levels relative to those found in the modern world remain poorly constrained, as is the effect on Early Paleozoic ecology and deep-ocean chemistry.

The Silurian Period is also known for its global abundance of carbonate platform ecosystems, particularly on the southern shelf of Baltica in the paleotropics, which covered a substantially greater portion of the seafloor than today. The reef communities found during the Silurian first appeared in the Middle Ordovician and were apparently not significantly affected by the terminal end-Ordovician and early Silurian glaciations (Copper, 2002; Calner, 2008), resulting in reefs being important habitats for diverse marine communities throughout the Early Paleozoic (Copper, 1994; Moberg and Folke, 1999). The marine carbonate rocks of Baltica have been extensively studied, using both biostratigraphy and stable isotope geochemistry. However, a largely unexplored and

* Corresponding author.
E-mail addresses: nmars008@ucr.edu (N.L. Marshall), glove@ucr.edu (G.D. Love), favosites@ukr.net (V. Grytsenko), andrey.bekker@ucr.edu (A. Bekker).

https://doi.org/10.1016/j.orggeochem.2022.104528
Received 29 July 2022; Received in revised form 10 November 2022; Accepted 13 November 2022
Available online 21 November 2022
0146-6380/Published by Elsevier Ltd.

unknown aspect of these marine ecosystems, especially for Baltica, is the composition of the microbial communities that underpinned food webs and mediated biogeochemical cycles. Detailed microbial lipid biomarker records for the marine realm are conspicuously sparse for the Silurian Period, especially the middle to late Silurian time interval. Relatively little is thus known about the broad structure of marine microbial communities through this period, such as the balance of bacterial versus eukaryotic organisms.

Previous organic geochemical investigations of rocks from the Silurian period have focused on biomarker fingerprinting to facilitate oil-source correlations and include studies from the Michigan Basin of USA (Gardner and Bray, 1984; Obermajer et al., 2000), North Africa and Arabia (Peters et al., 2005; Romero-Sarmiento et al., 2010, 2011; Diasty et al., 2017), and Lithuania (Zdanaviciute and Bojesen-Koefoed, 1997; Zdanaviciute and Lazauskiene, 2004, 2007). However, very few, if any, organic geochemical studies have focused on the microbial community structure that sustained Silurian marine ecosystems. In contrast, several detailed lipid biomarker studies over the past decade have characterized the microbial communities that sustained Early to Late Ordovician and Late Devonian ecosystems (Rohrssen et al., 2013; Haddad et al., 2016; Spaak et al., 2017; Lee et al., 2019; Martinez et al., 2019).

A distinctive and common lipid biomarker characteristic reported from Ordovician rocks and oils is an unusually high contribution of 3β-methylhopanes (3-MeH). These ancient 3β-methylhopanes are usually attributed to methanotrophic bacteria, particularly microaerophilic type I and type X methanotrophic proteobacteria, especially when they are found in high abundance in ancient rocks and oils (Collister et al., 1992; Ruble et al., 1994; Farrimond et al., 2004). Other bacterial sources of 3-MeH are feasible (Zundel and Rohmer, 1985; Welander and Summons, 2012; Kool et al., 2014; Mayer et al., 2021) under appropriate environmental conditions that favored growth of the source organisms. The most likely Paleozoic source biota for these biomarkers when found in the marine realm are discussed later (see Section 5.4).

Tropical carbonate reefs, especially those located on the southern shelf offshore of Baltica, were ancient marine habitats that hosted diverse and complex Silurian marine ecosystems (Bjerkéus and Eriksson, 2001; Copper, 2002; Tuuling and Flodén, 2013; Vinn et al., 2014). One of the aims of this study was to characterize broad features of microbial community structure, such as the balance and temporal variation of algal versus bacterial source contributions. Additionally, our investigation helps bridge a conspicuous gap in the ancient biomarker record through an important time interval in the history of life, associated with a major global environmental change inferred for rising levels of atmospheric oxygen and marine dissolved oxidants. Here, we present the first detailed Silurian biomarker stratigraphic records from the investigation of a > 400 m long drill core from Ukraine that spans the middle Silurian to Early Devonian time interval. The thermally well-preserved and carbonate-rich sediments from this drill core preserved diverse suites of lipid biomarkers that allowed us to study changes in source biota and marine carbon cycling on this ancient, tropical shallow-marine reef-rimmed carbonate platform during the late Silurian.

2. Geologic setting

Drill-core 25 (Fig. 1) was collared on the southwestern margin of Baltica on the bank of the Horyn River in Kotyuzhyny village (Ternopil District) of Podillya, Ukraine (49°54′35.5′′N, 25°50′20.0′′E) in November 2005. The sedimentary cover sitting on the Precambrian basement of Baltica in this area consists of the Neoproterozoic and Early to Middle Paleozoic (Cambrian to Carboniferous) strata (Kaljo et al., 2012; Radkovets, 2015). The Silurian and Early Devonian stratigraphic units of the southern Podillyan basin, intersected by drill-core 25, have been described previously (Tsegelnyuk, 1980; Grytsenko et al., 1983; Kaljo et al., 2012; Gozhik et al., 2013; Radkovets, 2015).The Silurian succession of Podillya has a stratigraphic hiatus at the base (Tsegelnyuk, 1980) and contains the late Llandovery and Přídolí stages, and continues into the Early Devonian.

The drill-core 25 succession has been lithostratigraphically correlated with that in the Dniester River region, 125 km to SW in Podillya, Ukraine, which is a classical area for the Silurian rocks and has been extensively studied (Baarli et al., 2003). The upper portion of the drill-core 25 has been correlated chemostratigraphically and biostratigraphically (e.g., based on graptolites) with numerous sections across Baltica (i.e., Western Lithuania; Western Latvia; SW Estonia; and Gotland) (Kaljo et al., 2007, 2012).

The stratigraphy and general lithofacies of drill-core 25 are described in detail by Kaljo et al. (2012). The drill core passed through the shallow-marine Wenlock to early Přídolí stages, represented by limestones and dolostones with thin beds and seams of gypsum and several bentonite beds. Stratigraphically higher, the Přídolí Stage succession became gradually more open marine with the Early Devonian limestones, marlstones, and mudstones lacking evaporite beds. The change from lithofacies that contain beds of gypsum to ones without has been related to a sea-level low stand that lasted through the Wenlock and earliest Přídolí stages. Later during the Přídolí Age, the Podillyan Basin experienced a continued transgression and deepening to lithofacies of limestones, marlstones, and mudstones lacking evaporites (Kaljo et al., 2012; Radkovets, 2015). The same sea-level pattern is also recorded in the Dniester river sections although the lithofacies are generally slightly deeper than those recorded by drill-core 25 (Kaljo et al., 2012). The depositional site of drill-core 25 during the Silurian to Early Devonian was a shallow-marine, episodically saline, lagoonal setting rimmed to the northwest by the reef tract (Grytsenko, 1987, 1993, 2007; Radkovets, 2015). Detailed description of the drill-core stratigraphy is provided in the Supplementary Materials.

A total of 26 samples were analyzed for biomarker hydrocarbons from drill-core 25, spanning 375.8 m of the drill-core length (every 14.4 m, on average). However, the upper portions of the drill-core were more closely sampled as they contain appreciably larger amounts of total organic carbon (TOC), making them more suitable for lipid biomarker analyses (> 0.1 wt% TOC).

3. Methods

3.1. Sample preparation

Samples were collected and transported in cloth bags. Outer portions of each drill core sample were removed with a water-cooled diamond saw and inner portions of the core were sonicated for 15 mins with deionized water (DI), dichloromethane (DCM), methanol (MeOH), *n*-hexane, and DCM. Each solvent rinse was discarded prior to rinsing with the next solvent. Cleaned rock samples were crushed using organic solvent-cleaned zirconia ceramic puck mill and dish housed within an 8515 SPEX shatterbox. Combusted quartz sand (pretreated at 850 °C for 9 h) blanks were run in parallel with the extracted rock powders as full analytical procedural blanks as an important control to monitor background levels and ensure that laboratory contaminant contributions to biomarker assemblages were negligible.

3.2. LECO total organic carbon (TOC) and Rock-Eval pyrolysis analyses

To determine TOC contents, the samples were decarbonated and analyzed on a LECO 230 instrument at GeoMark Research, using their standard protocol with concentrated HCl for at least two hours. The samples were then rinsed with water and flushed through a filtration apparatus to remove the acid. The filter was then removed, placed into a LECO crucible, and dried in a low temperature oven (110 °C) for a minimum of 4 h. The LECO C230 instrument was calibrated with standards that have known carbon contents. Standards were combusted by heating to 1200 °C in the presence of oxygen; both carbon monoxide (CO) and carbon dioxide (CO_2) were generated, and the CO was converted to CO_2 wuth a catalyst. The CO_2 product mass was measured with

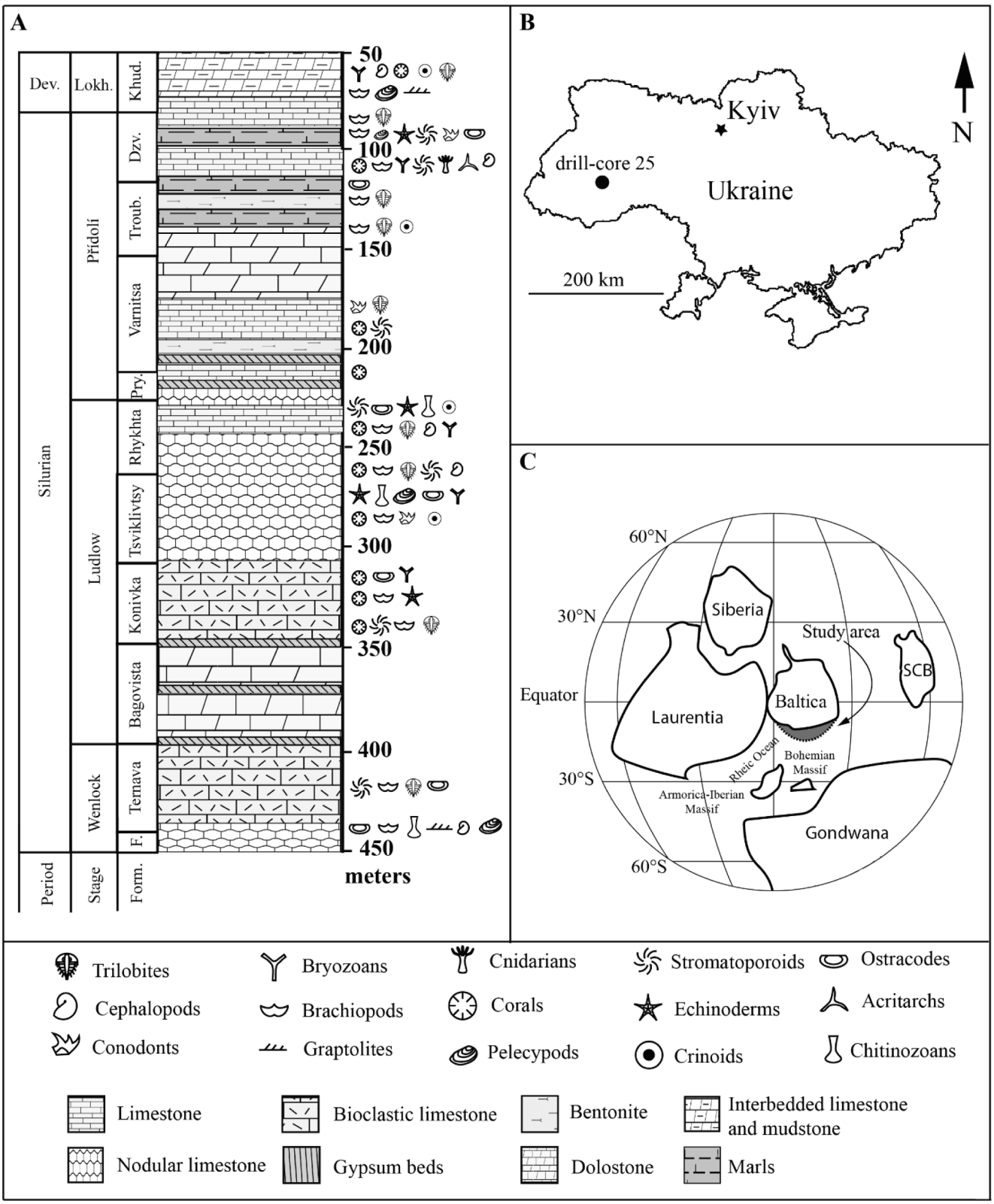

Fig. 1. Stratigraphic column (A) of the sampled Silurian-Devonian interval of drill-core 25: Dev – Devonian; Lokh – Lokhovian; Form – Formation; F – Furmanivka; Pry – Pryhorodok; Troub – Troubchin; Dzv – Dzvenigorod; Khud – Khudikivtsy. (B) Map showing location of the studied drill-core 25 in Ukraine. (C) Paleogeographic reconstruction of continents during the middle Silurian (Torsvik et al., 1996). SCB – South China Block.

an IR cell. Combustion of samples with unknown organic carbon content was then completed and the response of these samples per mass unit was compared to that of the calibration standard. Standards were analyzed every 10 samples to check variation and calibrate the analysis. An acceptable standard deviation for TOC is 3% variation from the established value. Instrument calibration was achieved using a rock standard with values determined from a calibration curve for pure hydrocarbons of varying concentrations.

Approximately 100 mg of washed, ground (60 mesh) whole rock sample were analyzed in a Rock-Eval II instrument. Measurements include S1: free bitumen content (mg HC/g rock), S2: remaining generation potential (mg HC/g rock), T_{max}: temperature at maximum evolution of S2 hydrocarbons (°C), and S3: organic carbon dioxide yield (mg CO_2/g rock), and were generated by heating according to the following parameters S1: 300 °C for 3 min; S2: 300 °C to 550 °C at 25 °C/min, and then held at 550 °C for 1 min; S3: trapped between 300 and 390 °C.

3.3. Solvent extraction and silica gel chromatography of rock bitumens

Typically, 5–20 g of rock powder per sample was extracted in organic solvent-cleaned Teflon vessels on a CEM MARS5 microwave accelerated reaction system in 30 ml of 9:1 (v/v) DCM/MeOH. Samples were heated to 100 °C for 15 mins with constant magnetic bar stirring. Procedural blanks were performed with combusted silica. Rock bitumens were recovered from vacuum filtration and elemental sulfur was removed with solvent-cleaned and HCl-activated copper granules. Saturated hydrocarbon, aromatic hydrocarbon, and polar (N, S, O) fractions were obtained through fractionation of rock bitumen on dry packed silica gel (Fisher, 60 grit) microcolumns. The silica gel was combusted in a muffle furnace at 450 °C for at least 9 h to remove any moisture and trace organic residue prior to adsorption of whole rock extracts and use in column chromatography. The saturated hydrocarbon fraction eluted with 1 dead volume (DV) of *n*-hexane, aromatic hydrocarbons with 3 DVs of 1:1 (v/v) *n*-hexane:DCM, and the polar hydrocarbons with 2 DVs of 3:1 (v/v) DCM:MeOH, respectively.

3.4. Gas chromatography–mass spectrometry (GC–MS)

The saturated and aromatic hydrocarbon fractions were run in full scan mode (*m/z* 50–800 Da) on an Agilent 7890A gas chromatograph (GC) system coupled to an Agilent 5975C inert MSD mass spectrometer. Samples were injected as hexane solutions in splitless injection mode with a programmable temperature vaporizing (PTV) inlet and using He as the carrier gas. The GC was equipped with a DB1-MS capillary column (60 m × 0.32 mm, 0.25 μm film thickness). The GC temperature program used for full scan analysis was 60 °C (held for 2 min), heated to 150 °C at 20 °C/ min, then to 325 °C at 2 °C/min, and held at 325 °C for 20 mins.

3.5. Metastable reaction monitoring GC–MRM-MS

The polycyclic alkane constituents of saturated hydrocarbon fractions were analyzed in detail by metastable reaction monitoring GC–MRM-MS using a Waters AutoSpec Premier mass spectrometer equipped with an Agilent 7890A GC. The GC was equipped with a DB1-MS capillary column (60 m × 0.25 mm, 0.25 μm film thickness) with He used as the carrier gas. The samples were injected as hexane solutions in splitless mode using an inlet temperature of 320 °C. The GC temperature program used for compound separation consisted of an initial hold at 60 °C for 2 min, then heated to 150 °C at 10 °C/min, then to 320 °C at 3 °C/min and finally held isothermally for 22 mins. Analyses were performed in electron impact mode with 70 eV ionization energy and 8 kV accelerating voltage. MRM transitions for C_{27}–C_{35} hopanes, C_{31}–C_{36} methylhopanes, C_{21}–C_{22} and C_{26}–C_{30} steranes, C_{30} methylsteranes and C_{19}–C_{26} tricyclics were selectively monitored in the method used. Procedural blanks with pre-combusted sand yielded < 0.1 ng of individual hopane and sterane isomers per gram of combusted sand. Polycyclic biomarker alkanes (tricyclic terpanes, hopanes, steranes, etc.) were quantified by addition of 50 ng of deuterated C_{29} sterane standard [d4-ααα-24-ethylcholestane (20R), Chiron Laboratories] to saturated hydrocarbon fractions and by comparison of relative peak areas. GC–MRM-MS was used to determine accurate biomarker abundance ratios for all the polycyclic biomarkers plotted in Figs. 2, 4, and 5. Analytical error for individual hopane and sterane concentrations are estimated to be ±30%. Average uncertainties in hopane and sterane biomarker ratios are ±8% as calculated from multiple analyses of saturated hydrocarbon fractions from in-house oil standards.

3.6. Catalytic hydropyrolysis (HyPy)

In addition to analysis of free hydrocarbon constituents in the rock bitumens amenable by solvent extraction, catalytic hydropyrolysis (HyPy) was performed on exhaustively extracted rock powders to generate products dominated by the kerogen-bound biomarker pool. This was used as an additional self-consistency check for ensuring that the free biomarker signals found are syngenetic with the kerogen in the host rocks. HyPy was performed on two extracted rock samples from middle and bottom (159 m and 300 m) of drill-core 25. This technique involves temperature-programmed heating of samples gradually from ambient temperature up to 520 °C in a continuous-flow configuration under high hydrogen gas pressure (15 MPa) to cleave covalent bonds and release the bound molecular constituents (Love et al., 1995), while preserving the original structural and stereochemical features of biomarker compounds to a high degree. Kerogen is an insoluble and immobile organic substrate; thus, it sequesters a significant pool of lipid biomarkers that can be released following covalent bond cleavage.

4. Results

All sedimentary rocks analyzed in this study contain an abundance of carbonate minerals, with an overall content ranging from 54 to 99 wt% of the bulk rock. The carbonate content was variable across the depth of the core. TOC content was generally low with an average value of 0.14 wt%, encompassing a range of 0.02–0.50 wt% of bulk rock. Thus, organic-lean, but fossiliferous carbonates are the dominant lithofacies in drill-core 25. The upper interval (85–140 m) records two global positive carbonate carbon isotope excursions during the Přídolí and Lochkovian stages (Kaljo et al., 2012). Despite this being a shallow-marine depositional setting, there was apparently sufficient connection to the open ocean to allow mixing of marine dissolved inorganic carbon into this inner ramp setting. It is therefore likely that the setting was open to the global ocean.

The high sensitivity and selectivity of GC–MRM-MS was utilized to generate strong polycyclic biomarker signals. The raw biomarker data, which includes the absolute biomarker yields for total hopanes, steranes, and methylhopanes as well as the biomarker abundance ratios used to construct Figs. 2, 4 and 5, are listed in the Supplementary Tables. The systematic changes seen in polycyclic alkane ratios downcore (Fig. 2) demonstrate the expected trend with increasing depth, whilst providing strong evidence that the lipid biomarker compounds detected are genuine Paleozoic biosignatures. These careful data verifications, along with parallel analysis of kerogen-bound distributions on two representative extracted rock samples from HyPy treatment (Section 4.2), are important self-consistency checks that were employed for ensuring that the biomarker hydrocarbon distributions are indeed syngenetic and endogenous organic constituents of the host rocks.

4.1. Thermal maturity proxies

Selected hopane and sterane maturity ratios (Fig. 2), used alongside standard temperature-programmed pyrolysis parameters (Supplementary Table S1), place these samples in the early- to mid-oil window range of thermal maturity. A consistently low thermal maturity profile, with

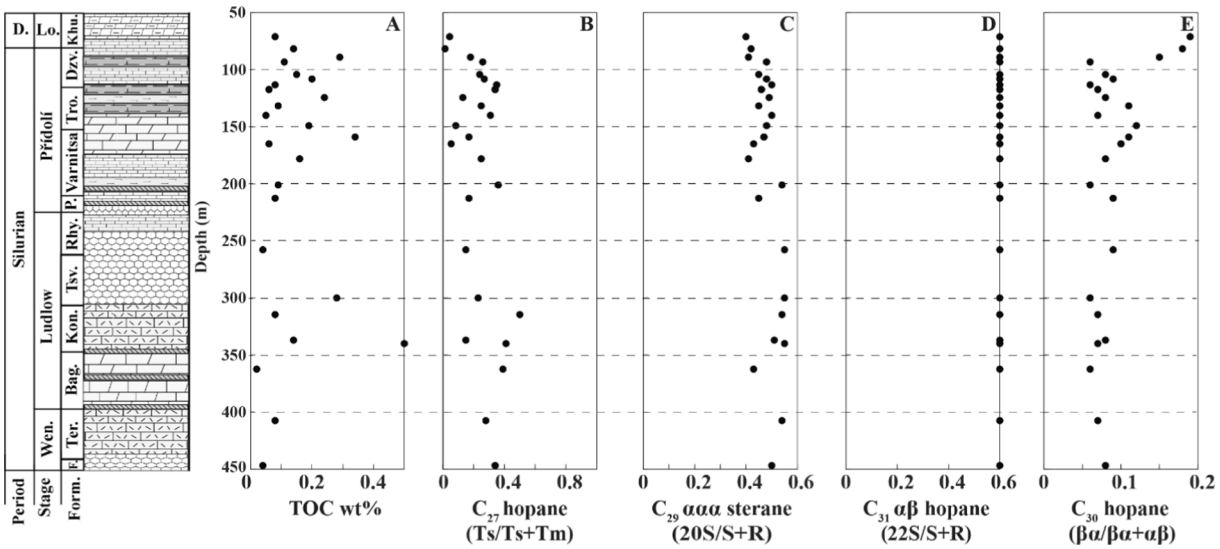

Fig. 2. Thermal maturity profile for drill-core 25 based on selected hopane and sterane maturity ratios. (A) Total organic carbon content (TOC; in weight precent); (B) C_{27} hopane (Ts/(Ts + Tm)); (C) C_{29} steranes (C_{29} αααS + αααR); (D) C_{31} αβ- hopanes (22S/(22S + 22R)); (E) C_{30} hopanes (C_{30} βα/(C_{30} βα + αβ)). D – Devonian; Lo – Lokhovian; Form – Formation; F – Furmanivka; P – Pryhorodok; Tro – Troubchin; Dzv – Dzvenigorod; Khu – Khudikivtsy.

slight systematic increases with depth, are observed through the succession. T_{max} values range from 430 to 443 °C. Hydrogen Index values (≤ 124 mg/g TOC and mostly < 100 mg/g TOC) are consistently low, signifying ancient rocks with poor oil-generating potential reflecting lipid-lean sedimentary organic matter deposited in oligotrophic marine settings. Given the low HI values, the bulk of the sedimentary organic matter is recalcitrant reworked kerogen, though polycyclic alkane analysis using GC–MRM-MS yielded strong biomarker signals (Fig. 3).

Further offshore in the Baltic Depression in Lithuania, graptolitic shales and marlstones were deposited in significantly more productive and deeper marine environments than for drill-core 25, in outer shelf to basinal settings (Zdanavicuite and Lazauskiene, 2007). In contrast to our data, Silurian marine source rocks from Lithuania of similar thermal maturity have higher TOC contents (≫1 wt%) and high HI values of 200–540 mg/g TOC, indicative of excellent oil-generating potential. Thus, the marine redox conditions and ocean productivity varied significantly across different regions in Baltica during the Silurian, with oligotrophic conditions more prevalent nearshore in lagoonal settings and eutrophic conditions sustained in some distal, open-marine settings.

Average values for C_{27} hopane (Ts/(Ts + Tm)) ratios are low at 0.24, which is typical for carbonate-rich rocks of this maturity. For extended hopanes, the average C_{31} αβ (22S/22S + 22R) ratio for side-chain epimerization of 0.60 ± 0.04 is a thermal equilibrium value expected for rocks that have reached oil window maturity. C_{29} ααα sterane (20S/(20S + 20R)) values of 0.48 ± 0.08 are found (Fig. 2) with a discernible systematic maturity increase with core depth: increasing from values of ca. 0.40 at the top of the core to ca. 0.55 in the deepest interval.

4.2. Catalytic hydropyrolysis (HyPy) of extracted sediments as an additional test for biomarker syngeneity

The bound steranes and hopanes released by HyPy exhibit a slightly less mature distribution of diastereoisomers than the corresponding free steranes and hopanes from two test samples (159 m and 300 m drill-core depth) due to enhanced protection of the bound biomarker pool by covalent binding within the macromolecular matrix (Supplementary Fig. S3). Rearranged stereoisomers (diasteranes and diahopanes) are clearly much less abundant and only trace constituents in the HyPy products compared with the corresponding free hydrocarbon fraction. This is the maturity offset and overall stereoisomer pattern typically found for kerogen-bound versus free systematic patterns expected for sedimentary organic matter of all geological ages that do not contain significant contamination contributions to the bitumen phase (Love et al., 1995, 2005, 2008). Similar sterane carbon number patterns (in this case, with a C_{29} dominance) are found for both the free hydrocarbon fraction and the corresponding HyPy products. In addition, both the 2α- and 3β-methylhopane distributions, from a shallow and deeper portion of the drill-core were analyzed for the products of the HyPy procedure (Fig. 3). The kerogen-bound biomarker pools yielded similar 2-MeHI and 3-MeHI index values, expressed as a percentage value [(C_{31} αβ MeH/(C_{31} αβ-MeH + C_{30} αβ-hopane)) × 100%], as found for the free hydrocarbon constituents in the bitumen extracts (see Fig. 3 and Supplementary Table S2). Thus, we are confident that the elevated 3β-methylhopanes abundances and other major biomarker stratigraphic patterns observed are primary signals.

4.3. Saturated hydrocarbon biomarker distributions and yields

Saturated hydrocarbon profiles generally contain abundant *n*-alkanes with a slight odd-over-even preference (OEP), especially prominent in the least mature intervals within the upper portions of the drill-core (Supplementary Fig. S1). Pristane and phytane are the dominant isoprenoids found and are likely sourced mainly from chlorophylls from phytoplankton. Methylalkanes are generally low in abundance relative to the dominant *n*-alkanes. The most abundant polycyclic biomarker alkanes include tri- and tetracyclic terpanes, steranes, hopanes, and methylhopanes, with hopanes being the dominant polycyclic compound series in all samples. Saturated hydrocarbons in samples with adequate yields of rock bitumen obtained from solvent extraction for full scan GC–MS analyses generally exhibited only low signal from unresolved complex mixtures (UCMs; see Supplementary Fig. S1).

Hopane/sterane ratios are variable throughout the studied drill-core but high values are commonly found (range: 1.4–37, mean: 10.7), which is a typical characteristic found previously for the Early Ordovician (Lee et al., 2019) and Middle-Late Ordovician carbonates (Rohrssen et al., 2013) deposited in oligotrophic settings. The range of H/St values found do not correlate with TOC content, which remains low (≤ 0.5 wt%) throughout the sedimentary succession.

The summed absolute concentrations of total steranes (C_{27}–C_{29} regular steranes and diasteranes) are low to moderate (0.5–111 ppm/TOC). C_{29} steranes are the dominant steranes in all but three samples, which is typical for Paleozoic rocks and oils (Schwark and Empt, 2006),

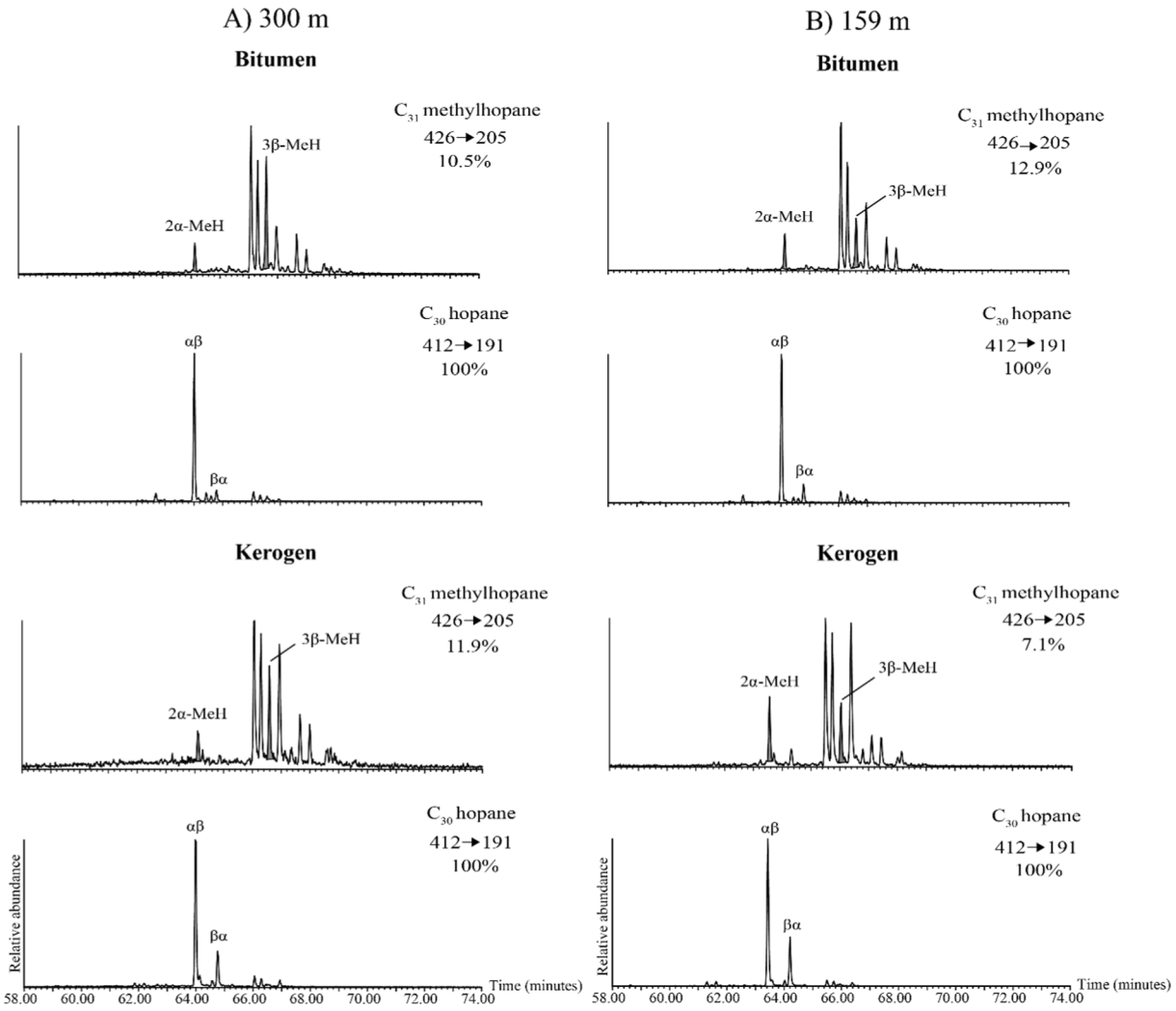

Fig. 3. GC–MRM-MS chromatograms for the free hopanes and methylhopanes alongside the kerogen-bound hopanes and methylhopanes for two samples from drill-core 25 (300 m and 159 m drill-core depth) with C_{30} hopanes (αβ and βα isomers) and C_{31} 2α- and 3β-methylhopanes (2α- and 3β-MeH, respectively) labeled. The peak signal in % is based on the relative peak intensity of the largest peak. Chromatograms show hopanes and methylhopane patterns generated for samples from: (A) 300 m drill-core depth; (B) 159 m drill-core depth samples from both the bitumen and kerogen phases.

followed by C_{27} and C_{28} steranes. C_{28}/C_{29} sterane ratios have a low average value of 0.4, but with a significant variation through the drill-core, encompassing a range of 0.17–0.81. C_{30} steranes are below reliable detection limits (< 0.3% of total C_{27}–C_{29} compounds) throughout the core and the main peaks detected in *m/z* 414 to 217 ion chromatograms are C_{30} diahopane and C_{30} αβ-hopane peaks from crosstalk rather than from genuine regular C_{30} sterane signals (Supplementary Fig. S2). Total C_{27}–C_{35} hopane abundances are significantly higher (9–289 ppm/TOC) compared with the concentrations of steranes. C_{29}/C_{30} hopane ratios are high (average = 0.89), which is typical for sedimentary rocks with high carbonate content (Peters et al., 2005).

Both 2α- and 3β-methylhopane homologs are present and readily detectable as the two resolvable methylhopane series using GC–MRM-MS. Methylhopane indices (MeHI) were calculated for the C_{31} homologs of 2α-methylhopane and 3β-methylhopane, expressed as a percentage value ((C_{31} αβ- MeH/(C_{31} αβ-MeH + C_{30} αβ-hopane) × 100%). 2α-Methylhopanes indices (2-MeHI) range from 1.3% to 5.7% with an average of 3.2%. The 2-MeHI abundances are consistent throughout the drill-core and show little to no correlation with TOC content. Absolute concentrations of 2α-methylhopanes range from 0.2 to 2.3 ppm/TOC. The 3-MeHI show a range of values from 3% to 13% with an average value of 6.4%, which is significantly greater than the Phanerozoic average of 1–3% (Rohrssen et al., 2013). Absolute concentrations of 3β-methylhopanes range from 0.13 to 5.5 ppm/TOC). The 3-MeHI are elevated throughout the drill-core, although the average is a bit lower in the Přídolí Stage and there is no obvious correlation with TOC content.

Fig. 4. shows that the gammacerane ratio (GM, calculated from relative peak areas of gammacerane/C_{30} αβ-hopane) exhibits very low values through the entire studied section. The extremely low GM ratios, from 0.01 to 0.08, are consistent with a normal marine salinity environment (Peters et al., 2005) having no appreciable redox or salinity stratification in the shallow-water column. Gypsum beds are found predominantly in the lower part of the drill-core, indicating evaporitic conditions. These sporadic episodes of elevated salinity were likely associated with shallow and oxic waters, precluding significant preservation of sedimentary organic matter during gypsum precipitation.

The homohopane index (HHI%; expressed as $C_{35}/(C_{31}–C_{35}) \times 100$) is another biomarker abundance parameter often used to assess the paleoredox depositional conditions. Under oxic depositional conditions, oxidative reactions facilitate cleavage and shortening of the extended hopane sidechain in bacteriohopanepolyols, favoring C_{31} hopanes over C_{35} hopanes (Farrimond et al., 2004; Peters et al., 2005). Very low values of HHI% (range: 0.29–6.2%, mean: 2.3%) are found throughout the drill-core, which indicates a pervasively well oxygenated marine environment consistent with mainly low productivity levels in a shallow-shelf setting.

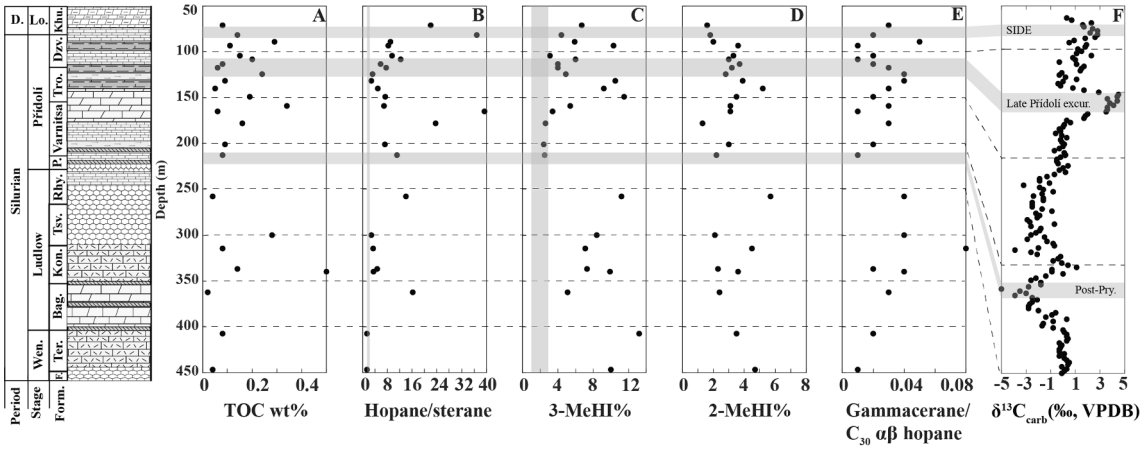

Fig. 4. Selected lipid biomarker ratios measured through drill-core 25. (A) Total organic carbon content (TOC; in weight percent); (B) Hopane/sterane (sum of C_{27}–C_{35} hopanes/sum of C_{27}–C_{29} diasteranes and regular steranes); (C) 3β-methylhopane index (3-MeHI%; C_{31} 3β-methylhopane/(3β-methylhopane + C_{30} αβ-hopane) × 100); (D) 2α-methylhopane index in percent (2-MeHI%; C_{31} 2α-methylhopane/(2α-methylhopane + C_{30} αβ-hopane) × 100) (E) Gammacerane ratio (Gammacerane/C_{30} αβ-hopane). (F) Replotted $\delta^{13}C_{carb}$ values from Kaljo et al. (2012) with gray shaded horizontal bars marking carbon isotope events. D – Devonian; Lo – Lokhovian; Form – Formation; F – Furmanivka; P – Pryhorodok; Tro – Troubchin; Dzv – Dzvenigorod; Khu – Khudikivtsy; Post-Pry. – Post-Pryhorodok low; Late Přídolí excur. – Late Přídolí excursion; SIDE – Silurian-Devonian boundary excursion. Gray shaded vertical bars in (B) and (C) represent the Phanerozoic marine average range values.

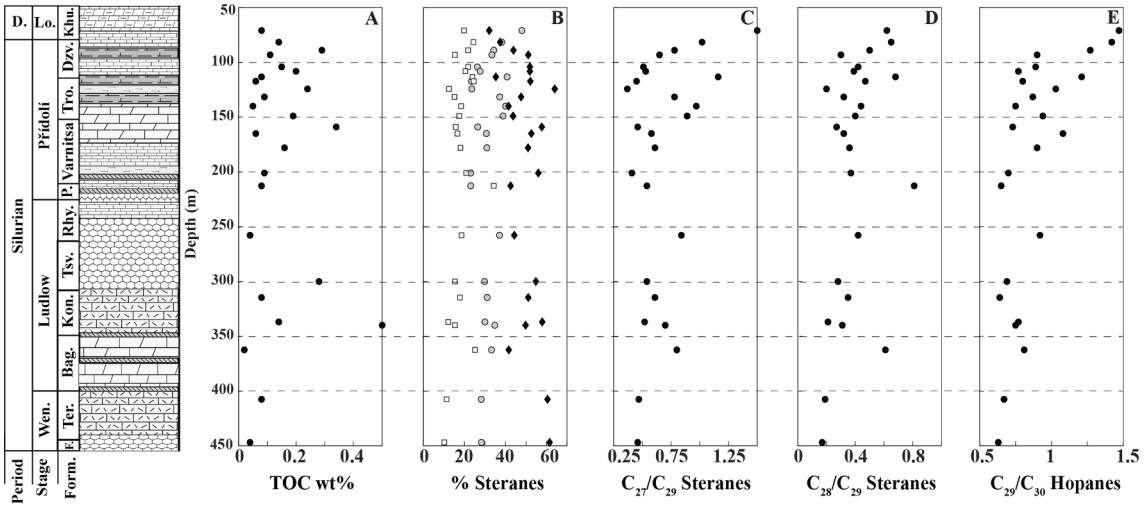

Fig. 5. Selected sterane and hopane biomarker ratios found in solvent extracts from drill-core 25 samples. (A) Total organic carbon content (TOC; in weight precent); (B) % steranes for C_{27} (filled circles), C_{28} (open squares), and C_{29} (black diamonds); % steranes for C_{27}, C_{28}, and C_{29}; (C) C_{27}/C_{29} steranes; (D) C_{28}/C_{29} steranes; (E) C_{29}/C_{30} hopane. D – Devonian; Lo – Lokhovian; Form – Formation; F – Furmanivka; P – Pryhorodok; Tro – Troubchin; Dzv – Dzvenigorod; Khu – Khudikivtsy.

5. Discussion

The upper part of the drill-core (254 m and above) has been chemostratigraphically and biostratigraphically (based mainly on graptolites) correlated with numerous sections across Baltica, therefore, the ages and stage boundaries are more certain for the upper part of the drill-core (Ludlow and Přídolí stages, Fig. 1; Kaljo et al., 2007, 2012). The lower part of the drill-core (below 254 m) has been lithostratigraphically correlated with the outcrop sections in the Dniester River area, which is a classical area with well-known biostratigraphically and lithostratigraphically characterized Silurian rocks (Baarli et al., 2003). The drill-core passed below the studied interval through the very thin Ordovician (typical for this area) and thick Cambrian sections further supporting the lithostratigraphically inferred Silurian age for the lower portion of the studied interval in the drill-core.

The biomarker distributions are expected to record the changing biological community structure, which evolved through time as the paleoenvironmental conditions were perturbed through sea level and climatic changes and other local and global factors. Local biomarker overprints and changes in biomarker assemblages through time are anticipated for any marine basin, but fluctuations in biomarker distributions are particularly acute for these semi-restricted inner shelf environments since water chemistry and biological communities are typically more variable over time than those in distal marine settings. Despite these complications, some first-order and consistent patterns are evident in drill-core 25 biomarker data. The lipid biomarker assemblages from the middle Silurian to Early Devonian carbonates from drill-core 25 clearly share some broad primary characteristics similar to those reported from Ordovician marine sedimentary rocks of various lithologies and from different marine depositional settings (Rohrssen et al., 2013, 2015; Spaak et al., 2017; Lee et al., 2019). Ordovician marine sedimentary rocks and oils usually exhibit some distinctive biomarker characteristics: elevated hopane/sterane ratios (often > 3 in organic-lean rocks), abundant 3β-methylhopanes from all rock lithologies, and

an absence and/or only trace abundances of regular C_{30} steranes. In this respect, the Silurian biomarker distributions from drill-core 25 are much more similar in composition to those typically found in Ordovician rocks than they are in comparison with the biomarker hydrocarbon assemblages reported thus far for Late Devonian sedimentary rocks (Haddad et al., 2016; Martinez et al., 2019).

5.1. Bacterially rich communities sustained Silurian, shallow-marine reef ecosystems

The ratio of the sum of all major hopane (C_{27}–C_{35}) versus sterane (C_{27}–C_{29}) constituents (H/St) gives a broad, but informative measure as to whether the balance of microbial communities, encompassing the major primary producers and consumers, was bacterially dominated or algal-rich. The Phanerozoic H/St average for organic-rich sedimentary rocks and oils derived from marine sediments deposited in nutrient-replete settings fall typically in the 0.5–2.0 (Rohrssen et al., 2013), signifying substantial eukaryotic source inputs. The H/St ratios found for most drill-core 25 samples are elevated (range: 1.4–39; mean: 10.3; most values > 3), implying a high bacterial contribution. The values of H/St ratios do not correlate with TOC content, which remains low ($\leq$ 0.5 wt%) throughout the sedimentary succession. The high proportion of bacterial source contribution to the preserved organic matter and the generally low TOC content for drill-core 25 have also been found previously for Ordovician rocks deposited in shallow, epeiric seaways at tropical paleolatitudes (Rohrssen et al., 2013; Lee et al., 2019).

The appreciable amounts of 2α-methylhopanes and 3β-methylhopanes imply that the high hopane series abundance in drill-core 25 was derived from mixed bacterial input, encompassing bacterial primary producers and methanotrophs as well as bacterial heterotrophs. Generally, bacterial picoplankton outcompete algae in nutrient-limited aquatic ecosystems, which only sustain low net biomass in oligotrophic marine settings of the modern ocean (Biddanda et al., 2001). The setting behind the reef tract in a lagoon and muted nutrient supply from the open ocean likely contributed to the persistently low primary productivity and low net biomass over millions of years of deposition on this carbonate platform through the Silurian. In contrast with drill-core 25, H/St ratios are low (0.3–1.0) in contemporaneous organic-rich shales and marlstones from Lithuania (TOC $>$ 1 wt%, ranging up to 19.2 wt%). The low H/St ratios in Lithuania are consistent with high algal productivity being sustained in nutrient-replete, open-marine conditions of deeper-water settings within the Baltic Depression (Zdanaviciute and Lazauskiene, 2007).

The major alkane constituents of the rock extracts from drill-core 25 are dominated by a marine *n*-alkane signal extending from C_{15} to C_{40} that begins to tail off in abundance with increasing carbon numbers above *n*-C_{23} or *n*-C_{25} (Supplementary Fig. S1). Samples demonstrate a slight, but discernible carbon number preference for odd-over-even carbon numbered *n*-alkanes in the C_{23} to C_{30} range in total ion chromatograms (TICs) from full scan GC–MS analysis (Supplementary Fig. S1). This abundance pattern is likely attributable to moderate green and other algal inputs superimposed on a bacterially sourced envelope of *n*-alkanes. Consistent with this strong bacterial contribution, hopanes [particularly C_{29} α β, C_{30} αβ, and C_{31} αβ (22S and 22R)] are the most abundant polycyclic alkane signals detected as major peaks in full scan TICs. The magnitude of the slight odd-over-even *n*-alkane preference is more pronounced in the upper core interval as expected, in part due to the lower thermal maturity of these host rocks preserving the original carbon number patterns to a slightly higher degree.

A homologous series of 2α-methylhopanes is present in all samples in moderate abundance, with an average value for 2-MeHI of 3.2% and a range of 1.3–5.7%. Biological precursors of 2α-methylhopanes are sourced mainly from cyanobacteria (Summons and Jahnke, 1990; Summons et al., 1999; Doughty et al., 2009; Welander et al., 2010; Naafs et al., 2022) and/or α-proteobacteria (Rashby et al., 2007; Welander et al., 2010; Naafs et al., 2022). The 2-MeHI values from drill-core 25 are hence assessed as moderate, especially for carbonate lithologies, which normally yield higher values than contemporaneous shales (Summons et al., 1999), but the ubiquity and appreciable amounts of 2α-methylhopanes mean that these are significant lipid biomarker constituents in the drill-core.

5.2. Sterane patterns for Silurian rocks compared to Late Ordovician and Devonian patterns

C_{29} steranes are commonly the most abundant steranes found in most Paleozoic marine rocks and oils (Grantham and Wakefield, 1988; Schwark and Empt, 2006), including Cambrian and Silurian samples that pre-date the radiation and expansion of vascular plants in the terrestrial realm with the Devonian. C_{29} steroids are preferentially produced by most green algal clades (Volkman et al., 1994; Kodner et al., 2008), consistent with green algae being the major eukaryotic marine phytoplankton in the Paleozoic Era. Some prasinophyte (green) microalgae can produce higher relative amounts of C_{28} steroids (Kodner et al., 2008), as well as abundant C_{29} steroids. In contrast, C_{27} and C_{28} are the most abundant steroids constituents of red algae, with rhodophytes producing a very strong C_{27} steroid dominance within their primary sterols (Kodner et al., 2008). Higher relative contributions of C_{28} steroids may also be sourced from red algal-derived lineages synthesizing chlorophyll *a* + c pigments, but these mainly radiated later in Mesozoic and younger oceans (dinoflagellates and coccolithophores initially, followed by diatoms during the Cretaceous and younger).

C_{29} steranes are commonly the most abundant sterane signal in most drill-core 25 samples with an average value of 49% (of total C_{27}–C_{29} sterane signal), although the C_{27} steranes become as abundant as C_{29} compounds in the upper two samples of the drill-core interval, which extends into the Early Devonian. The magnitude of C_{29} steranes dominance in the drill-core is generally not quite as pronounced as for Ordovician rocks. The abundance ratios of C_{28}/C_{29} steranes, which average 0.4 for the drill-core, reach values as high as 0.8, which is elevated compared to the typical Middle to Late Ordovician marine mean value of ~ 0.3 (Rohrssen et al., 2013). The enhanced contribution of C_{28} sterane biomarkers in a few samples of the drill-core could be due to an increased input of red algae (mainly C_{27} sterol producers) and/or C_{28} sterol-producing green algae from certain prasinophytes (Kodner et al., 2008); both of these scenarios result in diminished sterane contribution from C_{29} sterol-producing green algae.

The drivers governing the variability of the sterane distributions sourced from eukaryotic phytoplankton in the drill-core might be due to local factors, such as changes in local nutrient availability strongly tied to the temporal variation in the extent of basin restriction in this reef-rimmed, lagoonal depositional setting. Thus, we refrain from interpreting these temporal changes in sterane distributions as a global trend in major, marine eukaryotic phytoplankton occurring through the middle Silurian to Early Devonian. The changes in sterane carbon number patterns recorded in the drill-core are more likely due to a local environmental overprint superimposed on a strong green algal baseline signal (with C_{29} sterane preference being the major feature), reflecting the changing algal source contributions and environmental conditions in this shallow-water depositional setting through time.

5.3. Implications of extremely low/absent C_{30} regular steranes in middle to late Silurian marginal marine settings

The presence of the C_{30} sterane, 24-*n*-propylcholestane (24-npc), has most commonly been applied to distinguish Phanerozoic marine depositional environments, as opposed to lacustrine or highly restricted marine settings (Moldowan et al., 1990). This paleoenvironmental assessment has been applied by organic geochemists most commonly to the Devonian and younger geological records. Molecular clock estimates, from a time-calibrated molecular phylogeny constructed using sterol C-24 methyltransferase sequences, predict that marine

pelagophytes and their algal ancestors may not have first produced algal C_{30} sterols until the Devonian (Gold et al., 2016). Marine pelagophyte algae and their ancestors are hence the most likely the major source biota for 24-npc in Phanerozoic rocks and oils derived from Devonian and younger source rocks (Moldowan et al., 1990; Rohrssen et al., 2015; Gold et al., 2016), although foraminifera are another possible source of 24-npc (Grabenstatter et al., 2013).

The oldest occurrences of ancient 24-npc are found in the Cryogenian and Ediacaran rocks and oils from South Oman and Siberia (Love et al., 2008, 2009; Grosjean et al., 2009; Kelly et al., 2011; Lee et al., 2013), although this C_{30} sterane is absent/below detection limits in many contemporaneous Ediacaran rocks from Baltica (Pehr et al., 2018). The source of 24-npc in these Neoproterozoic rocks and oils might be from demosponges (Love et al., 2009) rather than from algae, since demosponges are the only modern taxa capable of biosynthesizing abundant sterols containing 24-npc, 24-isopropylcholestane (24-ipc), and 26-methylcholestane (26-mes), which are found together as three resolvable C_{30} sterane compounds in some Neoproterozoic rocks. Therefore, a major algal source of 24-npc steranes probably did not appear until well into the Paleozoic, which is compatible with molecular clock estimates (Gold et al., 2016).

A commonly found Ordovician hiatus in the occurrence of readily detectable 24-npc ($<$ 0.3% of total C_{27} to C_{29} steranes for reliable GC–MRM-MS detection limits) was reported previously by Rohrssen et al. (2015) from analysis of a suite of the Late Cambrian, Ordovician, and early Silurian sedimentary rocks. This Ordovician marine gap in 24-npc biomarker detection was later supported by analysis of Early Ordovician carbonates (Lee et al., 2019). In contrast, very few Silurian rocks and oils have been rigorously tested for 24-npc or other regular C_{30} sterane occurrences. We find here that 24-npc, 24-ipc and 26-mes are all below reliable GC–MRM-MS detection limits ($<$ 0.3% of summed C_{27} to C_{29} steranes) in our drill-core samples, which were deposited in a lagoonal setting on a reef-rimmed carbonate platform.

The absence of 24-npc may just be a local environmental feature rather than a consistent Silurian biomarker characteristic so caution must be applied at this stage. It is possible that algal sources of 24-npc first emerged during the Silurian, but only flourished in distal, open-marine settings, such as the outer shelf beyond the reef-rimmed carbonate platforms. Despite the sparse Silurian biomarker literature, this possibility is supported by the findings of Rohrssen et al. (2015), who reported low, but detectable 24-npc signal (0.3–0.8% of total steranes) in three analyzed early Silurian marine sedimentary rocks from Gotland, Sweden. Nutrient-limitation in the marginal-marine, reef-rimmed lagoonal setting where drill-core 25 strata were deposited made this habitat challenging for algae to flourish (see Section 5.1), which may account for the consistent absence of 24-npc signal. Thus, we need to be wary of extrapolating local sterane distributions to the entire Silurian marine sedimentary record. Thermally immature, Silurian rocks deposited in deeper-water, eutrophic marine settings should be targeted for future investigation.

5.4. Observed 3β-methylhopane trends through the late Silurian record systematic changes in Early Paleozoic marine methane cycling

Hopanes methylated at the C-3 position are typically minor compounds relative to the regular hopane series for most Phanerozoic marine rocks and oils, as reflected by the typical low values and range of 3-MeHI (1–3%) for most Devonian and younger marine rocks and oils (Rohrssen et al., 2013; Haddad et al., 2016; Martinez et al., 2019). 3β-Methylhopanes derived from 3β-methylbacteriohopanepolyols and/or 3β-methyldiploptene/diplopterol precursors are often associated with an origin from aerobic methanotrophic proteobacteria (Summons and Jahnke, 1990; Farrimond et al., 2004). Additionally, it has been found that an anaerobic methanotrophic bacterium, that utilizes nitrite as an oxidant, can synthesize 3-methylhopanoids in significant amounts (Kool et al., 2014). Thus, elevated abundances of 3-MeH sourced from bacterial methanotrophs are arguably the most likely dominant contributor of 3-MeH to ancient marine source rocks at circum-neutral seawater pH (Collister et al., 1992; Ruble et al., 1994; Farrimond et al., 2004), although other (mainly aerobic) bacterial sources of 3-MeH are possible (Welander and Summons, 2012). This source assignment is strongly supported by highly ^{13}C-depleted isotopic signatures characteristic of a methanotrophic origin for these compounds when found in particularly high abundance in ancient rocks (with high 3-MeHI values), such as reported for immature shales from the Green River Formation deposited in saline lake environment (French et al., 2020; Ruble et al., 1994; Collister et al., 1992). Other biogenic source contributions to ancient 3β-methylhopanes restricted to acidic paleoenvironments are acetic acid bacteria (Zundel and Rohmer, 1985) and one genus of anaerobic purple bacteria (Jahnke et al., 2014; Mayer et al., 2021), although such low pH-adapted organisms are not likely to thrive in marine and carbonate-dominated paleoenvironments.

Methanotrophic bacteria that synthesize 3-methylhopanoids oxidize methane to CO_2 with molecular oxygen (or use other oxidants such as nitrite; Kool et al., 2015) rely usually on a biogenic methane flux generated via methanogenesis in the water column and/or surface sediments as a carbon source. In modern marine sediments, methane oxidation largely occurs through the process of anaerobic oxidation of methane (AOM), although bacterial methanotrophy mediated mainly by type I methanotrophs occurs on the margins of the modern Eastern Tropical North Pacific oxygen-minimum zone (Chronopoulou et al., 2017). AOM in modern marine environments is the dominant process of methane sequestration consuming $>$ 90% of the annually produced methane before it can reach the water column or atmosphere (Knittel and Boetius, 2009; Thiel, 2018). The process of AOM is largely performed by a consortium of methane-oxidizing archaea and sulfate-reducing bacteria with sulfate being the final electron acceptor. Throughout most of the Paleozoic, low marine sulfate (Gill et al., 2007; Wu et al., 2014) and lower dissolved O_2 concentrations (relative to the Mesozoic and younger) likely promoted greater fermentative recycling of organic matter and an enhanced methane flux to the water column on continental margins from the locus of methanogenesis within oxygen-minimum zones (OMZs). Elevated 3β-methylhopane indices (3-MeHI) of ancient marine rocks, therefore, could signify enhanced, microbially driven (mainly aerobic) methane oxidation in marine shelf water columns, which were proximal to the margins of expansive OMZs (Rohrssen et al., 2013).

Previous research has demonstrated that Ordovician marine biomarker assemblages consistently exhibit elevated 3-MeHI values ($>$ 3%, and commonly ca. 4–18%) for a variety of lithologies and marine depositional settings, particularly from low-latitude sites (Rohrssen et al., 2013; Spaak et al., 2017; Lee et al., 2019). In contrast, Late Devonian and younger sedimentary rocks and oils appear to consistently yield much lower 3-MeHI values of ca. 1–3% (Haddad et al., 2016; Martinez et al., 2019) that may reflect an increasingly muted marine methane cycle and/or more oxygenated oceans. This might be related mechanistically to a contraction of OMZs in response to a Devonian rise of atmospheric oxygen and a concomitant increase in dissolved marine oxidants (Algeo et al., 2015; Haddad et al., 2016; Martinez et al., 2019; Stolper and Bucholz, 2019; Sperling et al., 2021), though the timing of any global-scale secular 3-MeHI change needs to be better constrained in the Phanerozoic.

Elevated 3-MeHI values (range: 3–13%, mean: 6.4%) are found throughout the drill-core. The 3-MeHI values do show a slight temporal decrease in magnitude through the Přídolí Stage and into the late Silurian–Early Devonian transition, compared with the underlying Silurian interval (Figs. 4 and 6). Given the sparseness of the Silurian biomarker record, the temporal trend of decreasing 3-MeHI moving stratigraphically up in the drill-core may reflect a local environmental change and not necessarily a widespread or global-scale trend. Despite this warranted caution, the values of 3-MeHI (4–10.3%) for the youngest strata deposited during the Silurian–Devonian transition are still

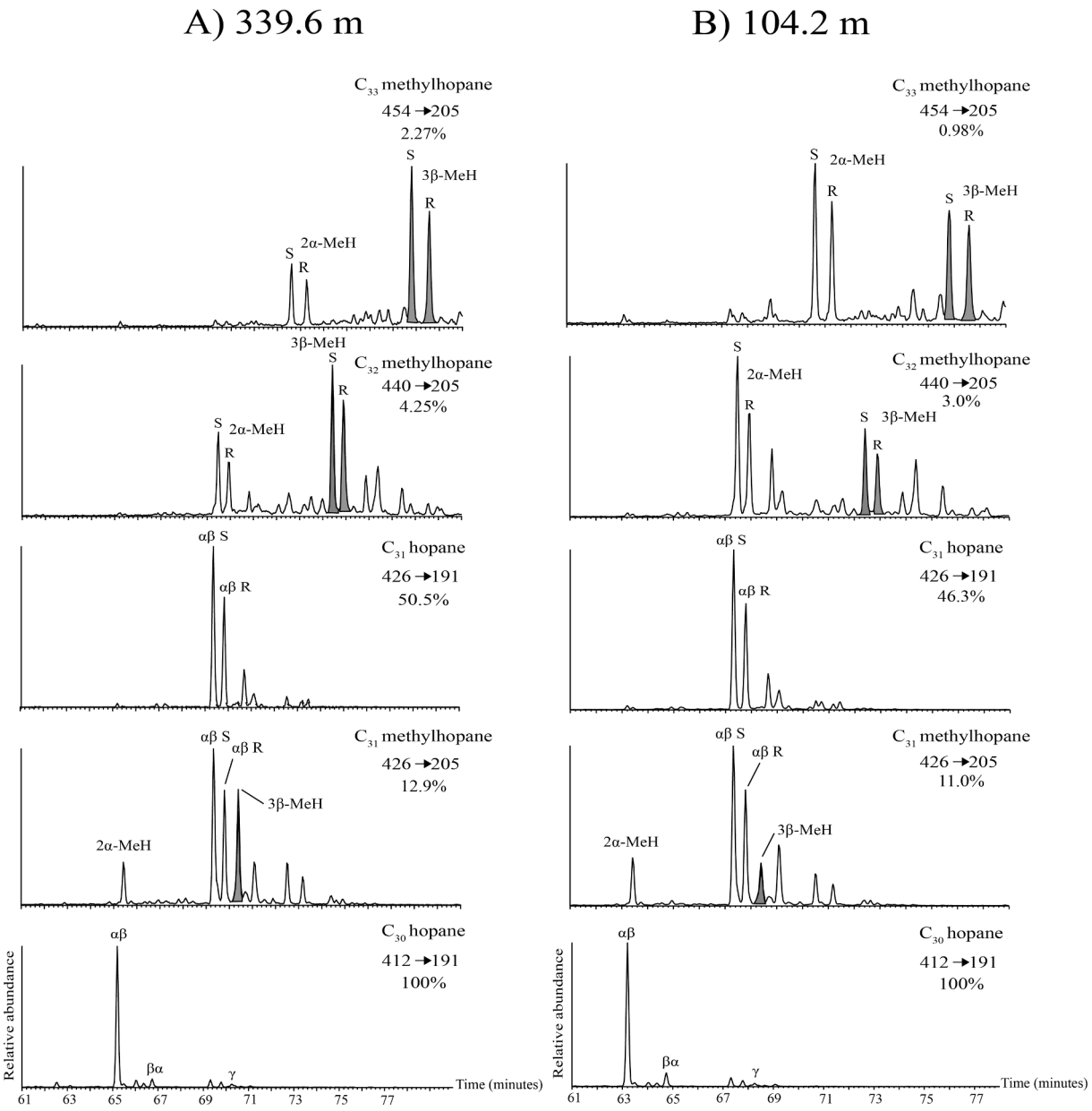

Fig. 6. Partial MRM ion chromatograms for selected samples from drill-core 25, comparing samples from 104.2 m and 339.6 m drill-core depth and highlighting the distributions and relative abundances of free hopanes and methylhopanes. The peak signal in % is based on the relative peak intensity of the largest peak. (A) C_{30} αβ and βα hopanes (white fill), γ = gammacerane; C_{31} 2α-methylhopane (light-gray fill); C_{31} αβ-(S and R) hopanes (white fill); C_{31} 3β-methylhopane (light-gray fill); (C) C_{31} αβ-(S and R) hopanes (light-gray fill); C_{32} 2α-methylhopanes (light-gray fill) and 3β-methylhopanes (light-gray fill); C_{33} 2α-methylhopanes (light-gray fill) and 3β-methylhopanes (light-gray fill).

consistently elevated in magnitude relative to younger Phanerozoic marine average values (1–3%). This result supports the interpretation that a vigorous marine methane cycle was sustained, at least locally at the southern margin of Baltica, for million years (Fig. 7). Bacterial methanotrophy, fueled by a biogenic methane flux delivered from deeper-water settings and shallow sediments which advected into shallow-marine waters, was likely a prevalent component of the marine carbon cycle on shelf settings during both the Ordovician and Silurian.

5.5. Implications of sustained bacterially dominated primary productivity on Silurian shallow marine environments for interpretating Silurian positive carbon isotope excursions on Baltica

Silurian carbon isotope stratigraphic records from Baltica have been well studied and show up to four major positive $\delta^{13}C_{carb}$ excursions across the period, many of which have now been globally correlated at multiple sites (Kaljo and Martma, 2006; Kaljo et al., 2007, 2012; Sadler, 2012; Hammarlund et al., 2019; Bowman et al., 2021; Hartke et al., 2021). The climatic and environmental context for these excursions remains up for debate, however one mechanistic driver proposed involves changes in thermohaline ocean circulation that shifted the locus of high primary productivity and carbon burial to distal marine settings (Jeppsson, 1990; Cramer and Saltzman, 2005; Calner, 2008; Munnecke et al., 2010) and affected ocean redox conditions. This would have impacted the global carbon isotope balance in favor a more ^{13}C-enriched dissolved inorganic carbon pool available for primary production for a significant period of geologic time (< 1 million years of duration) until strong negative biogeochemical feedbacks gradually restored to the pre-excursion baseline $\delta^{13}C_{carb}$ values of around 0‰.

Drill-core 25 strata were deposited in a reef-rimmed, lagoonal setting

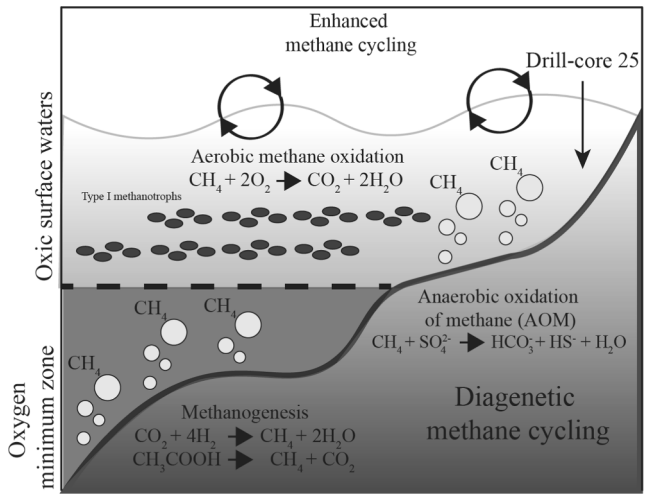

Fig. 7. A conceptional model for Silurian, tropical shelf environments as informed by the drill-core 25 biomarker study and previous Silurian biomarker investigation of graptolitic shales and marlstones from Baltic Depression in Lithuania (Zdanavicuite and Lazauskiene, 2007). The Silurian marine realm likely sustained enhanced marine methane cycling, operating in the water column and in sediments close to the sediment–water interface, enabled by low marine dissolved sulfate and O_2 concentrations in the Early Paleozoic.

and offer a unique opportunity to investigate the microbial ecology and redox conditions in Silurian marginal-marine settings. The mode of primary productivity, though somewhat variable, remained largely bacterially dominated throughout the depositional history of the drill-core. Additionally, there appears to be no fundamental shift in the TOC content of drill-core 25 marine sediments, with low TOC content prevalent. This characteristic along with the shallow-marine depositional setting and key biomarker features (low gammacerane ratio and low HHI) suggest that oxic environmental conditions on the inner shelf were maintained.

Across the interval of time that drill-core 25 spans at least one negative and two positive $\delta^{13}C_{carb}$ isotope excursions have been recognized across Baltica (Kaljo et al., 2007, 2012). The pair of positive $\delta^{13}C_{carb}$ excursions during the Přídolí Age (reaching up to +4‰) and across the Silurian-Devonian boundary (SIDE) have been recorded offshore of several continents. Both of these excursions are also captured in the carbonate carbon isotope record of drill-core 25 (Kaljo et al., 2012). It seems increasingly likely that the Silurian positive carbon isotope excursions were driven by changes in organic carbon cycling and organic matter burial in offshore marine settings, overriding biogeochemical processes which occurred in shallow, epeiric seaways and inner carbonate platform marine environments (Cramer and Saltzman, 2005; Hartke et al., 2021). This interpretation though requires further testing using a combination of high-resolution lipid biomarker and isotope stratigraphic records spanning through Silurian events.

6. Conclusions

Lipid biomarker records were generated for the > 400 m-thick middle Silurian to Early Devonian succession of sedimentary carbonates in drill-core 25 from Podillya, Ukraine (Baltica), deposited in a shallow-marine, reef-rimmed lagoonal tropical setting. This is the first detailed, stratigraphic Silurian biomarker study using GC–MRM-MS to resolve the distributions of the main biomarker hydrocarbon constituents. The biomarker assemblages suggest that organic-lean (with TOC $\leq$ 0.5 wt%) samples were deposited in a nutrient-depleted and shallow-marine, oxygenated environment with communities dominated by bacterial primary producers and consumers. High source contributions of bacteria are indicated by generally high hopane/sterane (H/St) ratio values (range: 1.4–37, mean: 10.7) for both the bitumen and kerogen phases, along with abundant methylhopanes. With respect to the main algal primary producers, the major regular steranes are mainly C_{29} from green algae, but with no appreciable contribution of any C_{30} regular sterane compounds. High 3β-methylhopane index (3-MeHI) values (mean: 6.4%, range: 3–13%) are consistently found throughout drill-core 25, which is a characteristic usually associated with significant inputs from methanotrophic bacteria. Our study extends the time span of consistently high 3-MeHI values, established for the Ordovician, to encompass Silurian marine environments.

Declaration of Competing Interest

The authors declare that they have no known competing financial interests or personal relationships that could have appeared to influence the work reported in this paper.

Data availability

Data will be made available on request.

Acknowledgments

NLM thanks UC Riverside for graduate fellowship funding. GDL is grateful to the Agouron Institute for grant support. GDL acknowledges a NASA Exobiology award (grant number 80NSSC18K1085) for funding this research. AB thanks Petroleum Foundation of the American Chemical Society for the grant 624840ND2. The authors acknowledge the constructive comments provided by two anonymous reviewers as well as John K. Volkman, Co-Editor-in-Chief.

Appendix A. Supplementary data

Supplementary data to this article can be found online at https://doi.org/10.1016/j.orggeochem.2022.104528.

References

Algeo, T.J., Luo, G.M., Song, H.Y., Lyons, T.W., Canfield, D.E., 2015. Reconstruction of secular variation in seawater sulfate concentrations. Biogeosciences 12, 2131–2151.
Baarli, B., Johnson, M., Antoshkina, A., 2003. Silurian stratigraphy and paleogeography of Baltica. New York State Museum Bulletin 493, 3–34.
Bassett, M.G., Siveter, D.J., Cocks, L.R.M., 1990. The Murchison Symposium. Journal of the Geological Society of London 147, 653–656.
Berner, R.A., 2009. Phanerozoic atmospheric oxygen: New results using the GEOCARBSULF model. American Journal of Science 309, 603–606.
Berner, R.A., Canfield, D.E., 1989. A new model for atmospheric oxygen over Phanerozoic time. American Journal of Science 289, 333–361.
Biddanda, B., Ogdahl, M., Cotner, J., 2001. Dominance of bacterial metabolism in oligotrophic relative to eutrophic waters. Limnology and Oceanography 46, 730–739.
Bjerkéus, M., Eriksson, M., 2001. Late Silurian reef development in the Baltic Sea. GFF 123, 169–179.
Bowman, C.N., Them, T.R., Knight, M.D., Kaljo, D., Eriksson, M.E., Hints, O., Martma, T., Owens, J.D., Young, S.A., 2021. A multi-proxy approach to constrain reducing conditions in the Baltic Basin during the late Silurian Lau carbon isotope excursion. Palaeogeography, Palaeoclimatology, Palaeoecology 581, 110624.
Calner, M., 2008. Silurian global events – at the tipping point of climate change. Mass Extinction. Springer. https://doi.org/10.1007/978-3-540-75916-4_4.
Chronopoulou, P.-M., Shelley, F., Pritchard, W.J., Maanoja, S.T., Trimmer, M., 2017. Origin and fate of methane in the Eastern Tropical North Pacific oxygen minimum zone. ISME Journal 11, 1386–1399.
Collister, J.W., Summons, R.E., Lichtfouse, E., Hayes, J.M., 1992. An isotopic biogeochemical study of the Green River oil shale. Organic Geochemistry, Proceedings of the 15th International Meeting on Organic Geochemistry 19, 265–276.
Copper, P., 1994. Ancient reef ecosystem expansion and collapse. Coral Reefs 13, 3–11.
Copper, P., 2002. Silurian and Devonian reefs: 80 million years of global greenhouse between two ice ages. Phanerozoic Reef Patterns 72, 181–238.
Cramer, B.D., Saltzman, M.R., 2005. Sequestration of ^{12}C in the deep ocean during the early Wenlock (Silurian) positive carbon isotope excursion. Palaeogeography, Palaeoclimatology, Palaeoecology 219, 333–349.
Diasty, W.S.E., Beialy, S.Y.E., Fadeel, F.I., Peters, K.E., Batten, D.J., 2017. Organic geochemistry of the Lower Silurian Tanezzuft Formation and biomarker characteristics of crude oils from the Ghadames Basin, Libya. Journal of Petroleum Geology 40, 299–318.

Doughty, D.M., Hunter, R.C., Summons, R.E., Newman, D.K., 2009. 2-Methylhopanoids are maximally produced in akinetes of *Nostoc punctiforme*: geobiological implications. Geobiology 7, 524–532.
Farrimond, P., Talbot, H., Watson, D.F., Schulz, L.K., Wilhelms, A., 2004. Methylhopanoids: Molecular indicators of ancient bacteria and a petroleum correlation tool. Geochimica et Cosmochimica Acta 68, 3873–3882.
Fisher, A.G., 1982. Long-term climatic oscillations recorded in stratigraphy. In: Berger, W.H. (Ed.), Climate in Earth History. National Academy of Sciences, pp. 97–104.
French, K.L., Birdwell, J.E., Vanden Berg, M.D., 2020. Biomarker similarities between the saline lacustrine Eocene Green River and the Paleoproterozoic Barney Creek Formations. Geochimica et Cosmochimica Acta, 274, pp. 228–245.
Gardner, W.C., Bray, E.E., 1984. Oils and source rocks of Niagaran reefs (Silurian) in the Michigan Basin. Petroleum Geochemistry and Source Rock Potential of Carbonate Rocks 18. https://doi.org/10.1306/St18443C3.
Gill, B.C., Lyons, T.W., Saltzman, M.R., 2007. Parallel, high-resolution carbon and sulfur isotope records of the evolving Paleozoic marine sulfur reservoir. Palaeogeography, Palaeoclimatology, Palaeoecology 256, 156–173.
Gold, D.A., Grabenstatter, J., de Mendoza, A., Riesgo, A., Ruiz-Trillo, I., Summons, R.E., 2016. Sterol and genomic analyses validate the sponge biomarker hypothesis. Proceedings of the National Academy of Sciences 113, 2684–2689.
Gozhik, P., Ivanik, M., Nemyrovska, T., Shevchuk, O., Veklych, O.D., Доротяк, Ю., 2013. Stratigraphy of Upper Proterozoic and Phanerozoic of Ukraine. Volume 1. Stratigraphy of Upper Proterozoic, Paleozoic and Mesozoic of Ukraine. Стратиграфія верхнього протерозою та фанерозою України. Стратиграфія верхнього протерозою, палеозою та Мезозою України. ІГН НАН України.
Grabenstatter, J., Méhay, S., McIntyre-Wressnig, A., Giner, J.-L., Edgcomb, V.P., Beaudoin, D.J., Bernhard, J.M., Summons, R.E., 2013. Identification of 24-*n*-propylidenecholesterol in a member of the Foraminifera. Organic Geochemistry 63, 145–151.
Grantham, P.J., Wakefield, L.L., 1988. Variations in the sterane carbon number distributions of marine source rock derived crude oils through geological time. Organic Geochemistry 12, 61–73.
Grosjean, E., Love, G.D., Stalvies, C., Fike, D.A., Summons, R.E., 2009. Origin of petroleum in the Neoproterozoic-Cambrian South Oman Salt Basin. Organic Geochemistry 40, 87–110.
Grytsenko, V.P., 1993. Silurian Period. In: Tsegelnyuk, P.D. (Ed.), Geological History of the Ukraine Territory. Paleozoic, Kyiv, Naukova Dumka, pp. 34–62 in Russian.
Grytsenko, V.P., Drygant, D.M., Ishchenko, A.A., Konstantinenko, L.I., Tsegelnyuk, P.D., 1983. The local Silurian scheme of Podolia. In: Sokolov B.S. (Ed.), The Silurian of Podolia. Academy of Sciences of the Ukrainian SSR, Kiev, 61–71. [WWW Document]. URL (accessed 4.14.22).
Grytsenko, V.P., 1987. Silurian shallow-water facies and corals of Volyn'-Podillya. Preprint of the Institute of Geological Sciences 87-21 of Sciences Ukrainian SSR, 34 pp.
Grytsenko, V., 2007. Distribution of corals on the Silurian Podolian Shelf. In: Hubmann, B., Piller, W.E., (Eds.), Fossil Corals and Sponges. Proceedings of the 9th International Symposium on Fossil Cnidaria and Porifera. Österr. Akad. Wiss., Schriftenr. Erdwiss. Komm. 17, 185–198.
Haddad, E.E., Tuite, M.L., Martinez, A.M., Williford, K., Boyer, D.L., Droser, M.L., Love, G.D., 2016. Lipid biomarker stratigraphic records through the Late Devonian Frasnian/Famennian boundary: Comparison of high- and low-latitude epicontinental marine settings. Organic Geochemistry 98, 38–53.
Hammarlund, E.U., Loydell, D.K., Nielsen, A.T., Schovsbo, N.H., 2019. Early Silurian $\delta^{13}C_{org}$ excursions in the foreland basin of Baltica, both familiar and surprising. Palaeogeography, Palaeoclimatology, Palaeoecology 526, 126–135.
Hartke, E.R., Cramer, B.D., Calner, M., Melchin, M.J., Barnett, B.A., Oborny, S.C., Bancroft, A.M., 2021. Decoupling $\delta^{13}C_{carb}$ and $\delta^{13}C_{org}$ at the onset of the Ireviken Carbon Isotope Excursion: $\Delta^{13}C$ and organic carbon burial (f_{org}) during a Silurian oceanic anoxic event. Global Planetary Change 196, 103373.
Jahnke, L.L., Turk-Kubo, K.A., N. Parenteau, M., Green, S.J., Kubo, M.D. y., Vogel, M., Summons, R.E., Des Marais, D.J., 2014. Molecular and lipid biomarker analysis of a gypsum-hosted endoevaporitic microbial community. Geobiology 12, 62–82.
Jeppsson, L., 1990. An oceanic model for lithological and faunal changes tested on the Silurian record. Journal of the Geological Society of London 147, 663–674.
Johnson, M.E., 1991. Silurian eustasy. In: Bassett, M.G., Lane, P.D., Edwards, D. (Eds.), The Murchison symposium–Proceedings of an International Conference on the Silurian system. Special Papers in Paleontology 44, 145–163.
Kaljo, D., Grytsenko, V., Martma, T., Mõtus, M.-A., 2007. Three global carbon isotope shifts in the Silurian of Podolia (Ukraine): Stratigraphical implications. Estonian Journal of Earth Sciences 56. https://doi.org/10.3176/earth.2007.02.
Kaljo, D., Martma, T., 2006. Application of carbon isotope stratigraphy to dating the Baltic Silurian rocks. GFF 128, 123–129.
Kaljo, D., Martma, T., Grytsenko, V., Brazauskas, A., Kaminskas, D., 2012. Pridoli carbon isotope trend and upper Silurian to lowermost Devonian chemostratigraphy based on sections in Podolia (Ukraine) and the East Baltic area/Susinikisotoopide suhte arengutrend Pridolis ja Ulem-Siluri ning Devoni alguse kemostratigraafia Podoolia (Ukraina) ja Baltikumi andmetel [WWW Document]. accessed 2.5.19 Estonian Journal of Earth Sciences. http://link.galegroup.com/apps/doc/A317309530/AONE?sid=googlescholar.
Kelly, A.E., Love, G.D., Zumberge, J.E., Summons, R.E., 2011. Hydrocarbon biomarkers of Neoproterozoic to Lower Cambrian oils from eastern Siberia. Organic Geochemistry 42, 640–654.
Knittel, K., Boetius, A., 2009. Anaerobic oxidation of methane: Progress with an unknown process. Annual Review of Microbiology 63, 311–334.
Kodner, R.B., Pearson, A., Summons, R.E., Knoll, A.H., 2008. Sterols in red and green algae: quantification, phylogeny, and relevance for the interpretation of geologic steranes. Geobiology 6, 411–420.
Kool, D.M., Talbot, H.M., Rush, D., Ettwig, K., Sinninghe Damsté, J.S., 2014. Rare bacteriohopanepolyols as markers for an autotrophic, intra-aerobic methanotroph. Geochimica et Cosmochimica Acta 136, 114–125.
Krause, A.J., Mills, B.J.W., Zhang, S., Planavsky, N.J., Lenton, T.M., Poulton, S.W., 2018. Stepwise oxygenation of the Paleozoic atmosphere. Nature Communications 9, 4081.
Lee, C., Love, G.D., Hopkins, M.J., Kröger, B., Franeck, F., Finnegan, S., 2019. Lipid biomarker and stable isotopic profiles through Early–Middle Ordovician carbonates from Spitsbergen, Norway. Organic Geochemistry 131, 5–18.
Lee, C., Fike, D.A., Love, G.D., Sessions, A.L., Grotzinger, J.P., Summons, R.E., Fischer, W.W., 2013. Carbon isotopes and lipid biomarkers from organic-rich facies of the Shuram Formation, Sultanate of Oman. Geobiology 11, 406–419.
Love, G.D., Snape, C.E., Carr, A.D., Houghton, R.C., 1995. Release of covalently-bound alkane biomarkers in high yields from kerogen via catalytic hydropyrolysis. Organic Geochemistry 23, 981–986.
Love, G.D., Bowden, S.A., Jahnke, L.L., Snape, C.E., Campbell, C.N., Day, J.G., Summons, R.E., 2005. A catalytic hydropyrolysis method for the rapid screening of microbial cultures for lipid biomarkers. Organic Geochemistry 36, 63–82.
Love, G.D., Stalvies, C., Grosjean, E., Meredith, W., Snape, C.E., 2008. Analysis of molecular biomarkers covalently bound within Neoproterozoic sedimentary kerogen. The Paleontological Society Papers 14, 67–83.
Love, G.D., Grosjean, E., Stalvies, C., Fike, D.A., Grotzinger, J.P., Bradley, A.S., Kelly, A. E., Bhatia, M., Meredith, W., Snape, C.E., Bowring, S.A., Condon, D.J., Summons, R. E., 2009. Fossil steroids record the appearance of Demospongiae during the Cryogenian period. Nature 457, 718–721.
Martinez, A.M., Boyer, D.L., Droser, M.L., Barrie, C., Love, G.D., 2019. A stable and productive marine microbial community was sustained through the end-Devonian Hangenberg Crisis within the Cleveland Shale of the Appalachian Basin, United States. Geobiology 17, 27–42.
Mayer, M.H., Parenteau, M.N., Kempher, M.L., Madigan, M.T., Jahnke, L.L., Welander, P. V., 2021. Anaerobic 3-methylhopanoid production by an acidophilic photosynthetic purple bacterium. Archives of Microbiology 203, 6041–6052.
Moberg, F., Folke, C., 1999. Ecological goods and services of coral reef ecosystems. Ecological Economics 29, 215–233.
Moldowan, J.M., Fago, F.J., Lee, C.Y., Jacobson, S.R., Watt, D.S., Slougui, N.-E., Jeganathan, A., Young, D.C., 1990. Sedimentary 24-*n*-propylcholestanes, molecular fossils diagnostic of marine algae. Science 247, 309–312.
Munnecke, A., Calner, M., Harper, D.A.T., Servais, T., 2010. Ordovician and Silurian sea–water chemistry, sea level, and climate: A synopsis. Palaeogeography, Palaeoclimatology, Palaeoecology 296, 389–413.
Naafs, B.D.A., Bianchini, G., Monteiro, F.M., Sánchez-Baracaldo, P., 2022. The occurrence of 2-methylhopanoids in modern bacteria and the geological record. Geobiology 20, 41–59.
Obermajer, M., Fowler, M.G., Snowdon, L.R., Macqueen, R.W., 2000. Compositional variability of crude oils and source kerogen in the Silurian carbonate–evaporite sequences of the eastern Michigan Basin, Ontario, Canada. Bulletin of Canadian Petroleum Geology 48, 307–322.
Pehr, K., Love, G., Kuznetsov, A., Podkovyrov, V., Junium, C., Shumlyanskyy, L., Sokur, T., Bekker, A., 2018. Ediacara biota flourished in oligotrophic and bacterially dominated marine environments across Baltica. Nature Communications 9. https://doi.org/10.1038/s41467-018-04195-8.
Peters, K.E., Walters, C.C., Moldowan, J.M., 2005. The Biomarker Guide. In: Biomarkers and Isotopes in Petroleum Systems and Earth History, vol. 2. Cambridge University Press.
Radkovets, N., 2015. The Silurian of southwestern margin of the East European Platform (Ukraine, Moldova and Romania): lithofacies and palaeoenvironments. Geological Quarterly 59. https://doi.org/10.7306/gq.1211.
Rashby, S.E., Sessions, A.L., Summons, R.E., Newman, D.K., 2007. Biosynthesis of 2-methylbacteriohopanepolyols by an anoxygenic phototroph. Proceedings of the National Academy of Sciences 104, 15099–15104.
Rohrssen, M., Love, G.D., Fischer, W., Finnegan, S., Fike, D.A., 2013. Lipid biomarkers record fundamental changes in the microbial community structure of tropical seas during the Late Ordovician Hirnantian glaciation. Geology 41, 127–130.
Rohrssen, M., Gill, B.C., Love, G.D., 2015. Scarcity of the C_{30} sterane biomarker, 24-*n*-propylcholestane, in Lower Paleozoic marine paleoenvironments. Organic Geochemistry 80, 1–7.
Romero-Sarmiento, M.-F., Riboulleau, A., Vecoli, M., Versteegh, G.J.M., 2010. Occurrence of retene in upper Silurian–lower Devonian sediments from North Africa: Origin and implications. Organic Geochemistry 41, 302–306.
Romero-Sarmiento, M.-F., Riboulleau, A., Vecoli, M., Versteegh, G.-J.-M., 2011. Aliphatic and aromatic biomarkers from Gondwanan sediments of Late Ordovician to Early Devonian age: An early terrestrialization approach. Organic Geochemistry 42, 605–617.
Ruble, T.E., Bakel, A.J., Philp, R.P., 1994. Compound specific isotopic variability in Uinta Basin native bitumens: paleoenvironmental implications. Org Geochem. 21, 661–671.
Sadler, P., Sadler, P., 2012. Integrating carbon isotope excursions into automated stratigraphic correlation: An example from the Silurian of Baltica. Bulletin of Geosciences 87. https://doi.org/10.3140/bull.geosci.1307.
Schwark, L., Empt, P., 2006. Sterane biomarkers as indicators of palaeozoic algal evolution and extinction events. Palaeogeography, Palaeoclimatology, Palaeoecology 240, 225–236.
Spaak, G., Edwards, D.S., Foster, C.B., Pagès, A., Summons, R.E., Sherwood, N., Grice, K., 2017. Environmental conditions and microbial community structure during the

Great Ordovician Biodiversification Event; a multi-disciplinary study from the Canning Basin, Western Australia. Global Planetary Change 159, 93–112.
Sperling, E.A., Melchin, M.J., Fraser, T., Stockey, R.G., Farrell, U.C., Bhajan, L., Brunoir, T.N., Cole, D.B., Gill, B.C., Lenz, A., Loydell, D.K., Malinowski, J., Miller, A.J., Plaza-Torres, S., Bock, B., Rooney, A.D., Tecklenburg, S.A., Vogel, J.M., Planavsky, N.J., Strauss, J.V., 2021. A long-term record of early to mid-Paleozoic marine redox change. Science Advances 7, eabf4382.
Stolper, D.A., Bucholz, C.E., 2019. Neoproterozoic to early Phanerozoic rise in island arc redox state due to deep ocean oxygenation and increased marine sulfate levels. Proceedings of the National Academy of Sciences 116, 8746–8755.
Summons, R.E., Jahnke, L.L., 1990. Identification of the methylhopanes in sediments and petroleum. Geochimica et Cosmochimica Acta 54, 247–251.
Summons, R.E., Jahnke, L.L., Hope, J.M., Logan, G.A., 1999. 2-Methylhopanoids as biomarkers for cyanobacterial oxygenic photosynthesis. Nature 400, 554–557.
Thiel, V., 2018. Methane carbon cycling in the past: Insights from hydrocarbon and lipid biomarkers. In: Hydrocarbons, Oils and Lipids: Diversity, Origin. Chemistry and Fate, Springer, pp. 1–30. https://doi.org/10.1007/978-3-319-54529-5_6-1.
Tsegelnyuk, P.D., 1980. Yarugskaya i malinovetskaya serii (nizhnij i verkhnij silur) Podolii i Volynii [The Yaruga and Malinovtsy series (the lower and upper Silurian) of Podolia and Volynia]. Preprint Institute of Geological Sciences, Academy of Sciences of the Ukrainian SSR, Kiev 53, 80–82. In Russian.
Tuuling, I., Flodén, T., 2013. Silurian reefs off Saaremaa and their extension towards Gotland, central Baltic Sea. Geological Magazine 150, 923–936.
Vandenbroucke, T.R.A., Emsbo, P., Munnecke, A., Nuns, N., Duponchel, L., Lepot, K., Quijada, M., Paris, F., Servais, T., Kiessling, W., 2015. Metal-induced malformations in early Palaeozoic plankton are harbingers of mass extinction. Nature Communications 6, 7966.
Vinn, O., Wilson, M.A., Mõtus, M.-A., 2014. Symbiotic endobiont biofacies in the Silurian of Baltica. Palaeogeography, Palaeoclimatology, Palaeoecology 404, 24–29.
Volkman, J.K., Barrett, S.M., Dunstan, G.A., Jeffrey, S.W., 1994. Sterol biomarkers for microalgae from the green algal class Prasinophyceae. Organic Geochemistry 21, 1211–1218.
Welander, P.V., Summons, R.E., 2012. Discovery, taxonomic distribution, and phenotypic characterization of a gene required for 3-methylhopanoid production. Proceedings of the National Academy of Sciences 109, 12905–12910.
Welander, P.V., Coleman, M.L., Sessions, A.L., Summons, R.E., Newman, D.K., 2010. Identification of a methylase required for 2-methylhopanoid production and implications for the interpretation of sedimentary hopanes. Proceedings of the National Academy of Sciences 107, 8537–8542.
Wu, N., Farquhar, J., Strauss, H., 2014. $\delta^{34}S$ and $\Delta^{33}S$ records of Paleozoic seawater sulfate based on the analysis of carbonate associated sulfate. Earth and Planetary Science Letters 399, 44–51.
Zdanaviciute, O., Bojesen-Koefoed, J.A., 1997. Geochemistry of Lithuanian oils and source rocks: A preliminary assessment. Journal of Petroleum Geology 20, 381–402.
Zdanaviciute, O., Lazauskiene, J., 2004. Hydrocarbon migration and entrapment in the Baltic Syneclise. Organic Geochemistry 35, 517–527.
Zdanaviciute, O., Lazauskiene, J., 2007. The petroleum potential of the Silurian succession in Lithuania. Journal of Petroleum Geology 30, 325–337.
Zundel, M., Rohmer, M., 1985. Prokaryotic triterpenoids. European Journal of Biochemistry 150, 35–39.